Journal of Hazardous Materials 175 (2010) 779–788

Contents lists available at ScienceDirect

Journal of Hazardous Materials

journal homepage: www.elsevier.com/locate/jhazmat

Carbons prepared from coffee grounds by H_3PO_4 activation: Characterization and adsorption of methylene blue and Nylosan Red N-2RBL

A. Reffas[a,b], V. Bernardet[a], B. David[a], L. Reinert[a], M. Bencheikh Lehocine[b], M. Dubois[c], N. Batisse[c], L. Duclaux[a,*]

[a] LCME, Polytech'Savoie, Université de Savoie, 73376 Le Bourget du Lac Cedex, France
[b] Laboratoire de l'Ingénierie des Procédés, d'Environnement, Département de Chimie Industrielle, Université Mentouri, Constantine 25000, Algeria
[c] LMI, CNRS, Université Blaise Pascal, 24 Avenue des Landais, 63177 Aubière Cedex, France

ARTICLE INFO

Article history:
Received 13 July 2009
Received in revised form 16 October 2009
Accepted 20 October 2009
Available online 30 October 2009

Keywords:
Coffee grounds
H_3PO_4 activated carbons
Surface chemistry
Porosity
Dye adsorption

ABSTRACT

Activated carbons were prepared by the pyrolysis of coffee grounds impregnated by phosphoric acid at 450 °C for different impregnation ratios: 30, 60, 120 and 180 wt.%. Materials were characterized for their surface chemistry by elemental analysis, "Boehm titrations", point of zero charge measurements, Infrared spectroscopy, thermogravimetric analysis (TGA); as well as for their porous and morphological structure by Scanning Electron Microscopy (SEM) and nitrogen adsorption at 77 K. The impregnation ratio was found to govern the porous structure of the prepared activated carbons. Low impregnation ratios (<120 wt.%) led to essentially microporous and acidic activated carbons whereas high impregnation ratios (>120 wt.%) yielded to essentially mesoporous carbons with specific surface areas as high as 925 $m^2 g^{-1}$, pore volume as large as 0.7 $cm^3 g^{-1}$, and neutral surface. The activated carbons prepared from coffee grounds were compared to a commercial activated carbon ($S_{BET} \sim 1400\ m^2 g^{-1}$) for their adsorption isotherms of methylene blue and "Nylosan Red N-2RBL", a cationic and anionic (azo) dye respectively. The mesoporous structure of the material produced at 180 wt.% H_3PO_4 ratio was found to be appropriate for an efficient sorption of the latter azo dye.

1. Introduction

Coffee is produced all over the world (for 2008, according to the "International Coffee Organization", the production of coffee amounted to about 680,000,000 tons). A portion of coffee grounds is recycled as materials for soil remediation or as adsorbents for odor. Nevertheless, most of the coffee grounds have to be carbonized before any use [1]. The amount of carbon dioxide produced by the combustion of 1000 g of coffee grounds is estimated to 538 g [1]. The valorization of food wastes into valuable materials without generating pollutants is a big challenge and recommended for an industrial sustainable development in order to preserve the environment.

As the demand for environmental protection increases every year, activated carbons are widely used in the industry for purification, separation, and recovery processes. Any inexpensive materials such as biomass waste: nutshell [2], pecan shell [3], apple peal [4], date pits [5] olive seed and stone [6], peach stone [7], corncob [8], coffee bean [9] and grounds [1,3,10–12], waste tea [13], bagasse [14], coconut shell [15] with a high carbon content can be used as a raw material for the production of activated carbon.

The chemical activation is often used to produce activated carbons (ACs) from biomass waste [1–15], lignin [16], and wood [17]. It involves pyrolyzing the feedstock in presence of a chemical activating agent such as H_3PO_4, $ZnCl_2$, KOH, etc. Among the activation agents, H_3PO_4 offers several advantages [16,18,19]: (i) a non-polluting character (compared to $ZnCl_2$), (ii) the elimination by leaching with water, and (iii) recycleability for further use after water washing. In addition, phosphoric acid which is commonly used for the preparation of carbon adsorbents from lignocellulosic products gives the possibility to develop microporous and/or mesoporous carbon with a specific surface area depending on the temperature of activation [17].

The aim of the present study is to prepare activated carbons based on coffee grounds as an agricultural byproduct precursor, for the depollution of water effluents contaminated by dyes from textile industry. Namane et al. [12] have prepared a 640 $m^2 g^{-1}$ activated carbon from coffee grounds by chemical activation with a mixture of $ZnCl_2 + H_3PO_4$. However, the impregnation ratio was not mentioned. Carbonaceous materials with a lower specific surface area (120 $m^2 g^{-1}$) were also produced from coffee grounds either at 800 °C in conventional (muffle) furnace under N_2 atmosphere [20] or in microwave furnace at 400 °C in air

* Corresponding author.
E-mail address: laurent.duclaux@univ-savoie.fr (L. Duclaux).

0304-3894/$ – see front matter © 2009 Elsevier B.V. All rights reserved.
doi:10.1016/j.jhazmat.2009.10.076

[1]. Despite their low adsorption uptakes, the samples prepared by microwave heating are able to better adsorb methylene blue, orange II, and gentiane violet dyes than the char obtained by conventional treatment [1]. Tsunoda et al. [10] have also prepared activated carbon by the carbonization of coffee grounds at 500 °C for 3 h in inert atmosphere followed by a physical activation by CO_2 gas at 750–800 °C (1–4 h) showing a ~0.3 $cm^3\,g^{-1}$ microporous volume and a type V adsorption–desorption isotherms of water vapor. The transformation of coffee grounds into activated carbons by chemical activation using KOH was reported by Evans et al. [3]. In this activation process, the coffee grounds were pyrolyzed at 750 °C, mixed with KOH, and heated at 800 °C leading to microporous activated carbon (2030 $m^2\,g^{-1}$ specific surface area).

In this paper, the preparation and characterization of mesoporous/microporous H_3PO_4 activated carbons from coffee grounds (namely CGACs for coffee grounds activated carbons) are reported and the adsorption properties are compared to a commercial activated carbon (CAC). The H_3PO_4 chemical activation method was used because of its one-step simple process, low activation temperature, high yield, short activation time, and high development of mesoporous surface area. The activation temperature was set at 450 °C because the carbons from plant species origin shows the highest specific surface area while they are obtained in the 450–500 °C temperature range [5,15,17,21,22].

2. Experimental

2.1. Materials

2.1.1. Activated carbons prepared from coffee grounds

Raw Arabica coffee grounds were washed with distilled water to eliminate the impurities (dust and water soluble substances) and dried at 50 °C for 48 h prior to their activation.

The dried coffee grounds were impregnated with a weighted amount of H_3PO_4 aqueous solution and heat treated at 450 °C in air atmosphere. The impregnation ratio (X_p, in wt.%) is defined as the ratio of the weight of H_3PO_4 (g) to the weight of precursor (g of dried coffee grounds). The physico-chemical properties of the activated carbons prepared with X_p = 30, 60, 120, and 180 wt.% (namely CGAC30, CGAC60, CGAC120 and CGAC180, respectively) were studied.

Dried coffee grounds (20 g) were impregnated for 2 h with phosphoric acid solutions (60 mL) to form slurries. The suspensions were sonicated 1 h in an ultrasound bath (40 kHz) and dried at 110 °C for 24 h. Samples were then heated 1 h at 450 °C (heating rate: 10 °C min^{-1}). The residual phosphoric acid was eliminated from the activated carbons by washing (at least two weeks) with distilled water into a Soxhlet extractor at 100 °C until no phosphate ions were detected in the water by a lead nitrate test. The samples were also analyzed by X-ray microanalysis to confirm the absence of residual phosphate particles. After drying at 110 °C for at least 3 h, the final material was then grounded and sieved to obtain particles with diameter <80 μm.

The "yield" of the activated carbons synthesis is defined as the ratio of the weight of the activated carbon after activation, washing and drying (w) to that of the dry coffee grounds (w_0) : yield% = $(w_1/w_0) \times 100$. The "burn off" is the weight loss percentage due to the activation step.

2.1.2. Commercial vegetal activated carbon

As comparison, a commercial activated carbon was studied in the same conditions than CGAC. The CAC (1.5 mm particles size from Merck) is produced from wood by steam-activation. This granular carbon was also grounded and sieved to obtain particles with diameter < 80 μm.

2.2. Characterization

The effect of the impregnating ratio (30, 60, 120, and 180 wt.%) on structure and chemical properties of CGACs was studied. The CGACs and CAC were firstly characterized for their surface chemistry by thermogravimetric analyses (TGA), infrared spectroscopy, pH measurement of the point of zero charge (pH_{PZC}), and semi-quantitative titrations of surface functional groups ("Boehm" method); and secondly for their adsorption properties by nitrogen adsorption at 77 K (total pore, mesopore and micropore volume, surface area, and average pore diameter), and methylene blue adsorption. The CGACs and CAC were finally compared for their adsorption of "Nylosan Red N-2RBL", an anionic – azo – dye used in Nylon (polyamide 6 and polyamide 6.6) dyeing.

2.2.1. pH of carbons in water suspension and pH_{PZC}

The pH of each activated carbon was measured in a distilled water suspension (12.5 mL) of 0.5 g of adsorbent after heating at 90 °C and then cooling to room temperature.

The pH_{PZC} was determined by the so-called pH drift method [23]. The pH of a deoxygenized suspension (N_2 bubbling during 1 h) of the activated carbon (0.15 mg) and NaCl aqueous solution (50 mL at 0.01 mol L^{-1}) was adjusted to successive initial values between 2 and 12. The suspensions were stirred 48 h under N_2 and the final pH was measured and plotted versus the initial pH. The pH_{PZC} is determined at the value for which $pH_{final} = pH_{initial}$.

2.2.2. Boehm titration

Boehm titrations quantify the basic and oxygenated acidic surface groups on activated carbons [24]. In this study, surface functional groups such as carboxyl (R–COOH), lactone (R–OCO), phenol (Ar–OH), carbonyl or quinone (RR′C=O) and basic groups were determined. Four different basic reagents were used: sodium ethoxide ($NaOC_2H_5$), sodium hydroxide (NaOH), sodium carbonate (Na_2CO_3) and sodium hydrogen carbonate ($NaHCO_3$). Surface functional groups were quantified by assuming that $NaOC_2H_5$ reacted with all groups; NaOH did not react with the RR′C=O groups; Na_2CO_3 did not react with RR′C=O and R–OH groups; and that $NaHCO_3$ only reacted with R–COOH groups. The carbon was also titrated by hydrochloric acid (HCl) in order to estimate the amount of bases within the material.

Experimentally, about 0.15 g of each sample (CGACs or CAC) was mixed in a closed polyethylene flask with 50 mL of a 0.01 mol L^{-1} aqueous reactant solution (NaOH, or Na_2CO_3, or $NaHCO_3$, or HCl). In case of $NaOC_2H_5$, only 0.1 g of carbons was added in 50 mL of 0.01 mol L^{-1} solutions. The mixtures were stirred for 48 h at constant speed: 150 rpm, at room temperature. Then, the suspensions were filtrated at 0.45 μm on membrane filters (Durapore®-Millipore). To determine the oxygenated group content, back-titrations of the filtrate (10 mL) were achieved with standard HCl (0.01 mol L^{-1}). Basic groups contents were also determined by back titration of the filtrate with NaOH (0.01 mol L^{-1}) after agitation of the activated carbon (150 mg) in HCl (0.01 mol L^{-1}) for 48 h.

2.2.3. Thermogravimetric analysis

In order to detect the effect of the phosphoric acid impregnation ratio used for the chemical activation on the mass loss, the CGACs and CAC samples were characterized by thermogravimetric analysis in a homemade apparatus equipped with a Mettler balance (±0.1 mg). About 200 mg of sample were heated from 25 to 450 °C with a heating rate of 10 °C min^{-1} under a nitrogen flow.

2.2.4. Infrared spectroscopy

Mid-infrared transmittance measurements of the activated carbons were carried out on a NICOLET 380 FT-IR spectrometer at

room temperature in the 400–4000 cm^{-1} wavenumber range, with a 2 cm^{-1} resolution. Pellets made of a mixture of 0.6 mg of activated carbon and 200 mg of KBr were pressed at 350 MPa, and oven-dried 48 h at 110 °C before analysis.

2.2.5. Elemental analysis and morphological structure

The C, H, N, O, S and P contents (mass %) of the activated carbons were measured by elemental analysis at the "Laboratoire Central d'Analyse du CNRS" (CNRS, France) through a combustion and evolved gas infrared analysis method. The qualitative elemental compositions of the activated carbons were confirmed by X-ray microanalysis. The surfaces of washed AC samples were characterized by Scanning Electron Microscopy (SEM) using a LEO Stereoscan 440 microscope in the backscattered electron mode, coupled with an energy dispersive spectrometer (Kevex Sigma).

2.2.6. N_2 adsorption–desorption at 77 K

The N_2 adsorption–desorption isotherms of the activated carbons were measured using an automatic adsorption instrument (ASAP 2020, Micromeritics) at liquid nitrogen temperature (77 K). Prior to measurements, carbon samples were degassed at 300 °C for 12 h under vacuum. The specific surface areas (S_{BET}) of the activated carbons were calculated using the Brunauer–Emmett–Teller (BET) equation by assuming the area of the nitrogen molecule to be 0.162 nm^2. The micropore volume and microporous surface area were determined by the *t*-plot method [23]. The external surface area (i.e., surface covered by the mesoporous and macroporous volume) was calculated by difference of the BET surface area and the microporous surface computed from the *t*-plot. The total pore volumes were estimated as the liquid volume of adsorbate adsorbed (N_2) at a relative pressure of 0.99. In addition, the pore size distribution (PSD) was determined by using the Barrett–Joyner–Halenda (BJH) method applied on the adsorption/desorption hysteresis loop assuming a model of cylindrical open-ended pores [26]. A Non-Local Density Functional Theory (NLDFT) method based on a model assuming a carbon slit-like pore geometry was used to estimate the pore size distributions. Data at $P/P_0 < 0.01$ were obtained using incremental fixed doses of 5 $cm^3\ g^{-1}$ (STP). The equilibration interval was set up at 30 s. The stability of low P/P_0 points was verified using different values of the DFT regularization method provided by the ASAP 2020 V3.01 software: no changes were observed on pore size distributions shapes, especially for micropores.

2.2.7. Adsorption: of methylene blue (MB), and Nylosan Red N-2RBL (NR)

Because of its size (1.43 nm × 0.61 nm × 0.40 nm), the well known methylene blue cationic dye ($[C_{16}H_{18}N_3S]^+$, Cl^-) is commonly used to probe the mesoporous volume of activated carbons by adsorption experiments [27]. Thus, methylene blue (Sigma–Aldrich, dye content ≥ 82%) adsorption was studied on CGACs and CAC. Adsorption studies were carried out with 100 mg of activated carbon samples introduced into 100 mL of MB solutions with different initial concentrations in the range 0–1000 mg L^{-1}. The pH of the suspensions were adjusted at pH 6, using nitric acid (1 mol L^{-1}) or sodium hydroxide (1 mol L^{-1}) solutions. The adsorption equilibrium of MB on materials was reached after 24 h of stirring at 25 °C and 300 rpm. After filtration (Whatman No. 5 paper filters), the MB equilibrium concentrations were determined by spectrophotometry at 665 nm (Shimadzu UV-2101PC).

The adsorption of the anionic dye Nylosan Red N-2RBL (purchased from Varian) was also studied in batch adsorption experiments. The main properties of NR (Fig. 1) are reported in Table 1.

The adsorption isotherms of NR were studied, at pH 4 for 24 h in batch experiments at 25 °C. This pH was chosen because it is the pH of the dying effluents containing Nylosan Red. Adsorption

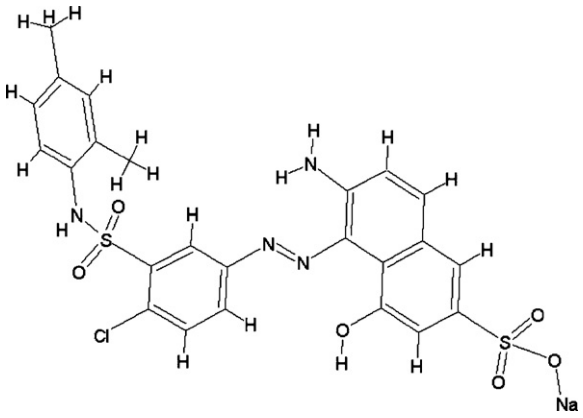

Fig. 1. Developed formula of Nylosan Red N-2RBL.

experiments were carried out with the same procedure than with the previous MB dye. After adsorption equilibrium, suspensions were filtrated on glass fiber filters (PALL, Type A/E, P/N 61631, pore size: 1 μm) and analyzed by UV–visible spectroscopy at 500 nm to determine the residual equilibrium dye concentration (C_e).

The equilibrium amount of MB and NR adsorbed on carbons (q_e in mg g^{-1}), was calculated by the following equations: $q_e = [(C_0 - C_e)V]/m$; where C_0 is the initial dye concentration (mg L^{-1}), C_e is the equilibrium dye concentration (mg L^{-1}), V is the volume of the solution (100 mL) and m is the mass of the adsorbent (g).

Adsorption isotherms of MB and NR were fitted by the Langmuir model using the linearized Langmuir equation: $C_e/q_e = 1/(k_L q_m) + C_e/q_m$; where k_L is the Langmuir constant and q_m (mg g^{-1}) is the maximum amount of dye which can be adsorbed. The maximum amount of adsorbed MB allows estimating the sample specific surface area covered by the MB molecule (S_{MB}) from the equation: $S_{MB} = q_m \times A_m \times 6.02 \times 10^{23}/M_{MB}$, with a molecular surface of MB (A_m) of 1.30 nm^2 and the 284 g mol^{-1} molecular mass of MB (M_{MB}) [28].

3. Results and discussion

3.1. Porous texture observed by N_2 adsorption/desorption at 77 K

Fig. 2 shows the N_2 adsorption–desorption isotherms of the activated carbons (CGACs and CAC). The isotherm of CGAC30 is typical of microporous materials (type Ia) where the micropore filling takes place at very low P/P_0 [25]. For CGAC60 and CGAC120, the isotherms are typical of microporous materials where the micropore filling takes place by co-operative process in wider micropores (type Ib) over a range of higher P/P_0 than in type Ia [25]. Nevertheless, for

Table 1
Properties of Nylosan Red N-2RBL.

Chemical name	Sodium 6-amino-5-[[4-chloro-3-[[(2,4-dimethylphenyl) amino] sulfonyl]phenyl]azo]-4-hydroxynaphthalene-2-sulfonate
C.A.S. number	71873-39-7
Color index: C.I.	Acid Red 336
Chemical formula	$C_{24}H_{21}ClN_4O_6S_2$,Na
Molecular weight (g mol^{-1})	587.97
Molecular size ($Å^3$)[a]	14.7 × 13.1 × 6.6
λ_{max} (nm)	500
pK_{a1}	6.8
pK_{a2}	9.2
pH (293 K, 10 g L^{-1})	10–11

[a] Value estimated by Chem3D software.

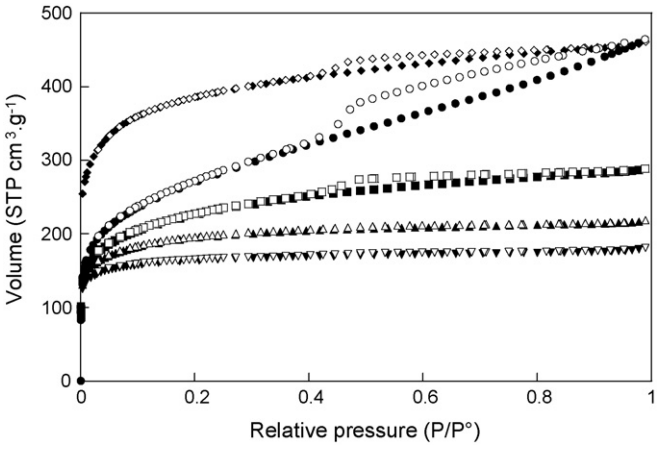

Fig. 2. N_2 adsorption (full symbol)/desorption (empty symbol) isotherms at 77 K on activated carbons: CGAC30 (▼), CGAC60 (▲), CGAC120 (■), CGAC180 (●) and CAC (♦).

CGAC120, the plateau is not clearly reached, indicating a widening of pores. The isotherm exhibits a type H_4 hysteresis loop, characteristic of slit-shaped pores. And finally, the CGAC180 and CAC show type IIb isotherms with an important adsorption at low P/P_0, and a type H_4 hysteresis loop, corresponding to the simultaneous presence of micro- and mesopores. The less pronounced hysteresis loop for CAC than for CGAC180 indicates that the mesoporous volume of this latter carbon is the largest.

The BET surface areas (S_{BET} = 514–925 $m^2\,g^{-1}$) reported in Table 2 can be favourably compared with other CGACs produced from coffee grounds [11,12] but are lower than the CAC (1440 $m^2\,g^{-1}$). The S_{BET} and external surface area increases together with X_p, slightly at low impregnation ratios and more steeply above 120 wt.%. By contrast, the micropore surface area deduced from *t*-plot decreases almost linearly from X_p = 30 to 180 wt.%. The CGACs are more or less microporous depending on the impregnation ratio (Table 2). As the impregnation ratio is increasing (Fig. 3), the microporous volume of the CGACs is decreasing and the mesoporous volume is increasing. As expected by the pronounced knee profile of their adsorption isotherms (Fig. 2), CGAC60 and CGAC120 are essentially microporous. Mesopores and macropores only represent ~40% of the total pore volume for CGAC30 and ~94% for CGAC180 (Fig. 3). As the amounts of H_3PO_4 increase, pores with a wide range of sizes are developed. At X_p higher than 60 wt.%, as the CGACs become predominantly mesoporous, the total and mesoporous volumes significantly increase (Fig. 3).

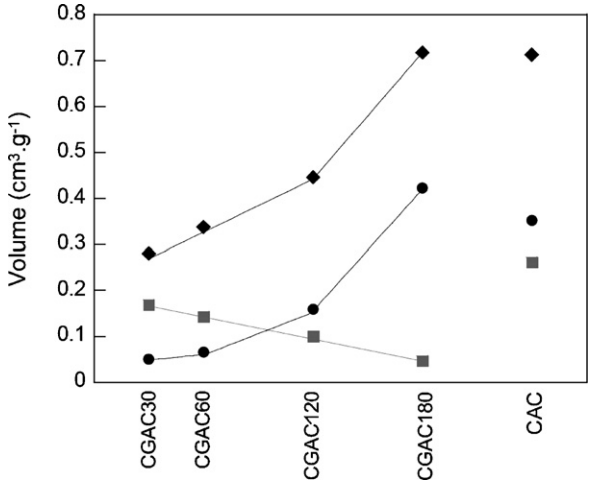

Fig. 3. Pore volume of the activated carbons (depending on X_p in wt.% for the coffee grounds CGACs): total (♦), microporous (■) and mesoporous (●) volumes (from *t*-plot and BJH adsorption model).

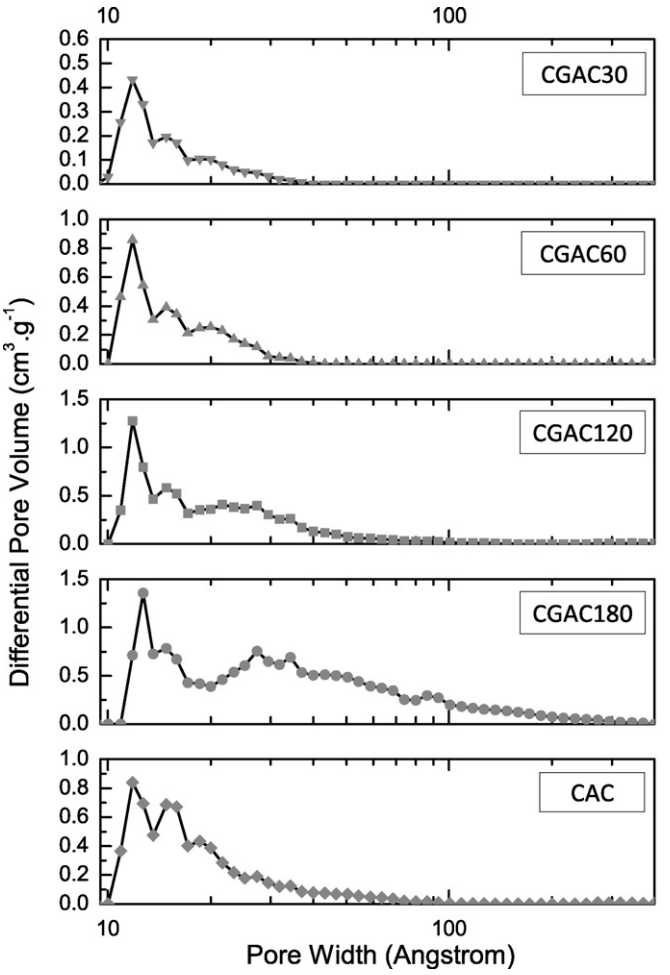

Fig. 4. Differential pore size distribution computed from DFT of the CGACs: CGAC30 (▼), CGAC60 (▲), CGAC120 (■) and CGAC180 (●) and commercial activated carbons (CAC: ♦).

CGAC180 and CAC possess quite the same porous volumes but the mesoporous volume of CGAC180 is slightly higher (Fig. 3). Fig. 4, illustrating the DFT pore size distributions (PSD), shows that the CAC mainly exhibits pores of diameter lower than 3 nm while the CGAC180 presents a distribution shifted towards larger pore sizes (>3 nm). DFT PSDs confirms that the pore sizes become predominantly mesoporous at impregnation degree higher than 120 wt.% while the materials prepared at lower ratios are mainly microporous.

Similar effects of the amount of phosphoric acid on porosity development have been reported for other lignocellulosic precursors [4,17,22]. As previously reported [17] for the activation process, the H_3PO_4 reacting within the internal cellulose structure is assumed to induce a depolymerization leading to an enhancement of the pore volume and thus a global volume expansion. In addition, as the amount of H_3PO_4 acid used for activation increases, the volume filled by it and the various associated polyphosphates is also enhanced, resulting in a larger pore volume and pore size, favouring the formation of mesopores [17]. The CGAC180 which possesses a high mesopore content might be an excellent adsorbent for the organic pollutants of middle molecular size (>2 nm).

Table 2
Textural properties obtained by N_2 adsorption/desorption studies.

Carbon parameters		CGAC30	CGAC60	CGAC120	CGAC180	CAC
Total surface area S_{ext} S_{BET} ($m^2\ g^{-1}$)	BET[a]	514	618	745	925	1440
Microporous surface area ($m^2\ g^{-1}$)	*t*-Plot	311	243	158	60	638
External surface area S_{ext} ($m^2\ g^{-1}$)	*t*-Plot	202	376	587	864	802
Mesoporous surface area ($m^2\ g^{-1}$)	BJH desorption[b]	103	205	417	821	495
Total pore volume ($cm^3\ g^{-1}$)	Single-point adsorption[c]	0.280	0.338	0.446	0.718	0.713
Microporous volume ($cm^3\ g^{-1}$)	*t*-Plot	0.169	0.143	0.100	0.046	0.262
	DFT	0.182	0.203	0.195	0.211	0.368
Mesoporous volume ($cm^3\ g^{-1}$)	BJH desorption[b]	0.066	0.124	0.279	0.666	0.331

[a] Computed in the P/P_0 range 0.05–0.30.
[b] BJH (Barrett Joyner Halenda) cumulative surface area of pores between 17 and 1000 Å diameters.
[c] At P/P_0 = 0.99 for CAC and CGACs.

Table 3
Production yield and burn-off after chemical activation of CGACs versus the orthophosphoric acid impregnation ratio.

X_p H_3PO_4 impregnation ratio (wt.%)	30	60	120	180
Production yield of carbons (%)	37.7	37.3	35.2	32.0
Burn-off (or mass loss; %)	62.3	62.8	64.7	67.9

3.2. Production yield and burn-off

The production yields (Table 3) are higher than those of a simple carbonization of the same material (9.5%) indicating the ability of H_3PO_4 to retain carbon material and to avoid the loss of otherwise volatile materials. The activation yields of CGACs in the range 38–32% (Table 3) indicates that the decomposition of coffee grounds was enhanced further by increasing the acid impregnation ratio. They are quite comparable to literature data on other adsorbents from agricultural wastes activated by phosphoric acid at 450 °C [29]. The weight losses ("burn-off") due to the heat treatment at 450 °C (Table 3) are in the same order of magnitude (close to 62–68%) and slightly increasing together with the impregnation ratio.

The transformation from lignocellulosic materials into carbon required evolving O and H atoms into H_2O, CO, CO_2, CH_4, aldehydes, etc., coupled to the distillation of heavier hydrocarbons (tar) [17,30]. Thus, the activation yield (and "burn-off") depends on the amount of carbon removed by binding with O and H atoms. The lower yield: 32% (∼68% "burn-off" for CGAC180) obtained with the highest impregnation ratio is caused by the enhancement of carbon burning-off by the excess of H_3PO_4 widening micropore into mesopore. Thus, the volatile matter content evolving from the chemically activated carbon depends not only on the temperature of pyrolysis [17] but also on the impregnation conditions [29]. As expected, the total porous volume of CGACs is related to the activation mass loss and linearly increases with the "burn off" value.

3.3. Surface chemistry

3.3.1. Morphology of materials and elemental analysis

Table 4 show that CGACs contain mainly carbon (68–76%), and oxygen (13–20%) with few amount of nitrogen (2%), hydrogen (3%) and phosphorus (1%). As the impregnation ratio increases, the carbon content increases, whereas the oxygen content decreases from 20% for CGAC30 to 13% for CGAC180. The content of hydrogen slightly increases, and the phosphorous one slightly decreases as the amount of activation agent increases. Compared to the CGACs, the CAC (Table 4) contains the highest amount of carbon and the lowest content of heteroatoms (6% of O) so that its surface is less acidic.

Table 4
Results of the elemental analysis of CGACs and CAC (mass %).

Element	CGAC30	CGAC60	CGAC120	CGAC180	CAC
P (%)	1.5	1.3	1.2	1.0	<0.04
C (%)	68.7	71.2	73.2	75.8	86.6
N (%)	2.4	2.1	2.2	2.0	0.7
H (%)	3.0	3.18	3.20	3.29	<0.3
O (%)	20.7	17.8	17.7	13.5	6.2
S (%)	<0.2	<0.2	<0.2	<0.2	0.2

The energy dispersive X-ray microanalysis (SEM/EDS) of the CAC (not shown) indicates mainly the presence of carbon (∼80%) but also of some heteroatoms, such as K, Na and Si originating from the wood precursor.

The SEM secondary electron images of 30, 60 and 120 wt.% CGACs are almost similar, and they show relatively heterogeneous surfaces as illustrated in Fig. 5 for CGAC30. By contrast the CGAC180 SEM image (Fig. 5) displays a few macropores (2–5 μm diameter) and more smooth surfaces. The CAC SEM surface image (Fig. 5) shows a quite homogeneous surface. As no particles of H_3PO_4 washing residue were observed by SEM; the presence of the P systematically detected (by EDS) in CGACs whatever their impregnation ratio, is due to P atoms bonded to local oxygenated surface or C atoms during the activation process.

3.3.2. pH, pH_{PZC} and surface functional groups

The pH of the material suspensions, the pH_{PZC} as well as the oxygenated group contents obtained by titrations are reported in Table 5.

The values of pH are quite similar to the values of pH_{PZC} whatever the activated carbon (Table 5). The pH_{PZC} values of CGAC30, CGAC60 and CGAC120 are close to 3.7. Both pH_{PZC} values of CAC and CGAC180 are higher than those of the former CGACs, and equal to 9.8 and 7.4 respectively. The CAC is rather a basic carbon in agreement with its low content of oxygen. The almost neutral value of the

Table 5
Surface chemical characteristics of the activated carbons.

Carbon	CGAC30	CGAC60	CGAC120	CGAC180	CAC
Carboxylic groups ($meq\ g^{-1}$)	0.466	0.390	0.266	0.266	0.000
Lactonic groups ($meq\ g^{-1}$)	0.200	0.200	0.234	0.014	0.000
Phenolic groups ($meq\ g^{-1}$)	0.709	0.700	1.033	0.786	0.416
Carbonyl groups ($meq\ g^{-1}$)	0.125	0.133	0.124	0.434	0.934
Total oxygenated groups ($meq\ g^{-1}$)	1.500	1.312	1.657	1.500	1.350
Total basic groups ($meq\ g^{-1}$)	0.000	0.000	0.000	0.000	1.466
pH	3.7	3.6	3.6	6.9	9.7
pH_{PZC}	3.7	3.6	3.9	7.4	9.8

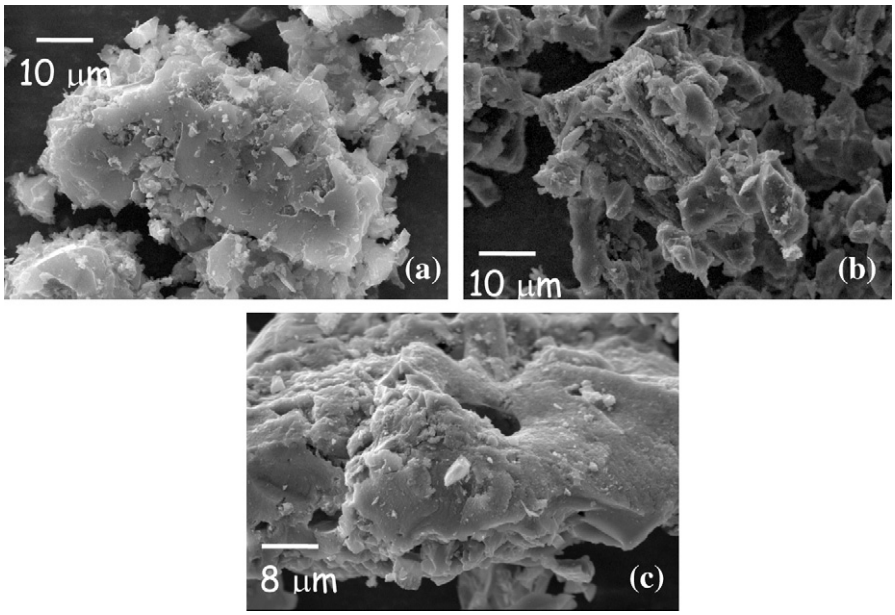

Fig. 5. SEM images of the CAC (a), CGAC30 (b), and CGAC180 (c).

pH_{PZC} for CGAC180 (7.4) compared to others CGACs ($pH_{PZC} \sim 3.7$), can be attributed to the increase of the phosphoric acid impregnation ratio to a certain level which results in decreasing the oxygen content at the surface (Table 4).

The "Boehm" titrations of CAC (Table 5) show less acidic than basic groups confirming its basic character. The CGAC30, CGAC60, and CGAC120 contain mainly phenolic and carboxylic groups (Table 5) explaining their acidic character. Increasing the impregnation ratio to 180 wt.% leads to a decrease in the content of lactonic groups (almost null) and carboxylic groups, and to a dramatic increase in the carbonyl content (Table 5). Thus, the neutral pH and pH_{PZC} of CGAC180 can be attributed to the presence of oxygenated surface groups with higher pK_a values by comparison with the others prepared activated carbons (pK_a-carboxylic ~ 4–5; pK_a-phenolic ~ 10; pK_a-carbonyl ~ 16–20).

3.3.3. Thermogravimetric analysis

The mass loss thermograms (measured in air) of coffee grounds (not shown) show four steps: (1) below 150 °C, the mass loss is due to a dehydration of materials; (2) the second step ($150 < T < 450$ °C), which corresponds to the primary carbonization, shows a greater mass loss (55%) due to the main volatile matters and tars elimination at 450 °C; (3) for $450 < T < 550$ °C, the mass decrease is due to the carbonization of coffee grounds; (4) at $T > 550$ °C the material is almost totally carbonized (mass loss = 96.5%). The ash content of the coffee grounds is then close to 3.5% in agreement with the CGACs elemental analyses which reports a 3–4% mass content of inorganic elements (deduced from Table 4).

TGA plots of CAC and CGACs (Fig. 6) show a first mass loss above 150 °C, attributed to the elimination of water physisorbed in the micropores and mesopores. This weight loss is higher than 15% for impregnation degrees lower than 120 wt.% and reaches 8% for CGAC180 and CAC confirming that these carbons are less hydrophilic in good agreement with their low oxygen surface contents (Tables 4 and 5).

The second small mass loss observed at the plateau between 170 and 450 °C can be interpreted in term of a decomposition of the oxygenated surface groups. These mass losses are equal to 1.75%, 1.76% and 1.51% for CGAC30, CGAC120 and CGAC180, respectively, and ~1% for CGAC180 and CAC. This mass loss is in agreement with the small amount of oxygenated functional groups determined by Boehm titration method (Table 5) and the low content of oxygen detected by elemental analysis (Table 4) in these latter carbons.

3.3.4. IR spectroscopy studies

The infrared spectra of CGACs and CAC are illustrated in Fig. 7. The more intense bands are reported in Table 6. The broad absorption band at 3300–3600 cm^{-1} with a maximum at about 3400 cm^{-1} is characteristic of the stretching vibration of hydrogen-bonded hydroxyl groups (from carboxyls, phenols or alcohols) and water adsorbed in the activated carbons (Fig. 7A). The broad band at ~3150 cm^{-1} only observed for CGAC30 and CGAC60 (Fig. 7b and c) is attributed to N–H bending vibrations (in amide). The absence of this IR band is consistent with the slight decrease in nitrogen element (Table 4) observed as the ratio of phosphoric acid increases up to 120 wt.%.

The FT-IR spectra of the commercial activated carbon and CGAC180 show absorption bands at 2930 and 2860 cm^{-1} arising from aliphatic C–H stretching in an aromatic methoxyl group, in methyl and methylene groups of side chains. The ν(C–H) stretching bands at 2930 and 2860 cm^{-1} (C–H stretching in –CH–) are

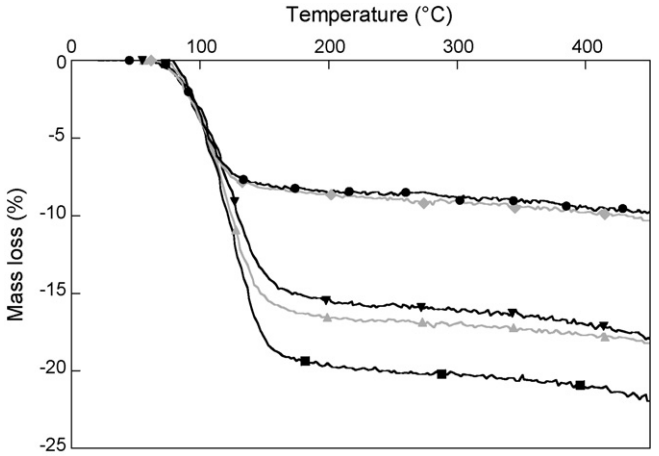

Fig. 6. Mass losses (%) versus temperature (°C) obtained by TGA under nitrogen atmosphere for CAC (◆), CGAC30 (▼), CGAC60 (▲), CGAC120 (■), and CGAC180 (●).

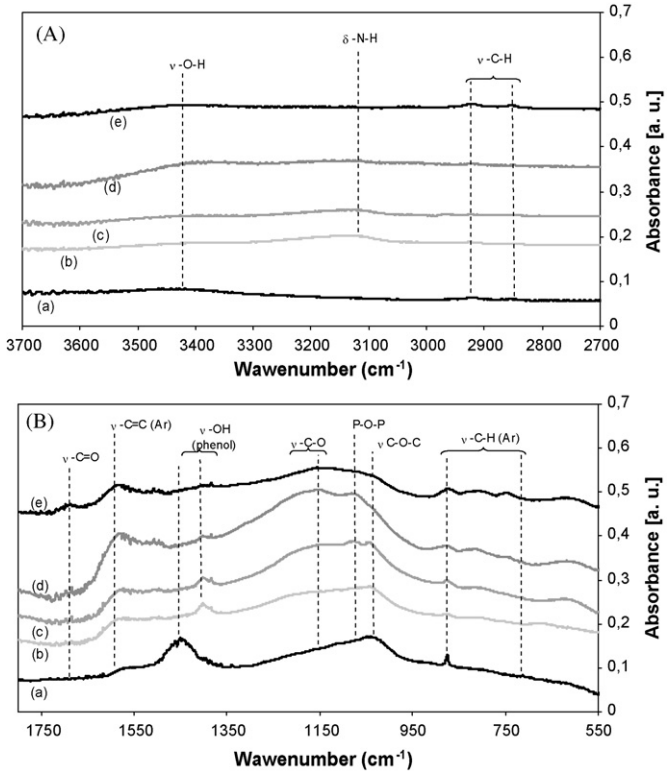

Fig. 7. (A and B) FT-IR spectra of activated carbons: CAC (a), CGAC30 (b), CGAC60 (c), CGAC120 (d), and CGAC180 (e).

detectable for the CGACs prepared at low impregnation ratios (30, 60, and 120 wt.%). In Fig. 7B, the bands at 885, 818, 756, 700 cm^{-1} are due to out-of-plane deformation mode of C–H for different substituted benzene rings. These bands are broadened as increasing the impregnation ratio.

The small band at about 1700 cm^{-1} is usually assigned to C=O stretching vibrations of ketones, aldehydes, lactones or carboxyl groups. The intensity of this band is increasing together with the phosphoric acid ratio in agreement with "Boehm" titrations (Table 5). Taking into account that the acid character is decreasing for CGAC180 (Table 5), the high intensity of the carbonyl IR band in this material and the absence of complementary characteristic bands of carboxylic acid and aldehydes suggests the presence of ketone groups.

The spectra of the CGACs and CAC carbon also show a strong band at 1600–1580 cm^{-1} due to C=C vibrations in aromatic rings.

Table 6
Infrared bands of CAC and CGACs.

Wavenumber (cm^{-1})	Assignment[a]	Wavenumber (cm^{-1})	Assignment[a]
3400	υ (O–H)	1200	υ_{as} (=C–O–C)
3150	υ (N–H)	1165	υ (C–O)
2930, 2860	υ (C–H)	1080	υ (P–O—P), υ ($P–O^+$)
1700	υ (C=O)	1050	υ_{as} (C–O–C)
1590	υ (C=C), aromatic ring	885, 818, 756, 700	γ (C–H)
1510	υ (C–C), aromatic ring	618	γ (O–H)
1450	δ_{as} (CH_3, CH_2 scissor)		
1450, 1400	δ (O–H)		
1390	δ_s (CH_3)		

[a] υ: stretching; δ: bending (in-plane); γ: bending (out-of-plane); s: symmetric; as: asymmetric.

The 1400 cm^{-1} region gives some idea of the relative abundance of CH_2 and CH_3 groups. The strong band at ~1450 cm^{-1} observed on the spectrum of CAC can be assigned both to the CH_2 bending vibrations and/or to the O–H bending band supported by the existence of phenols as this activated carbon does not contain carboxylic groups. However, this band is not observed in the CGACs which contain higher amounts of phenolic groups. The O–H bending band is assumed to be observed at ~1400 cm^{-1} in the CGACs and it decreases as increasing impregnation ratio as expected by the loss of acidic character previously observed by pH measurement and titrations (Table 5). A characteristic absorption of the methyl group (CH bending vibrations in CH_3) is observed at 1390 cm^{-1} in each CGACs spectrum.

All spectra (Fig. 7) also show a broad band in the main fingerprint spectral region between 1300 and 900 cm^{-1} with maxima at 1050, 1080 and 1165 cm^{-1} for CGACs. Broad band at 1000–1300 cm^{-1} is usually found with oxidized carbons and has been assigned to C–O stretching in acids, alcohols, phenols, ethers and esters. Nevertheless, it is also a characteristic of phosphorus and phosphocarbonaceous compounds present in the phosphoric acid activated carbons [31]. Assignment in this region is difficult because absorption bands from are overlapped. The shoulder at 1070–1080 cm^{-1} was ascribed to ionized linkage $P^+–O^-$ in acid phosphate esters [31] and to symmetrical vibration in a P–O–P chain [32]. These bands are well defined as the H_3PO_4 impregnation ratio increases and absent in CAC prepared by steam activation. In the region 900–1300 cm^{-1} the CAC IR spectrum shows a maximum at 1050 cm^{-1} and a shoulder at 1165 cm^{-1}. The maximum at 1050 cm^{-1} is also observed for CGACs and is less pronounced for CGAC180. The intensity evolution of this latter band which is attributed to C–O–C asymmetric stretching, is consistent with the lactone concentrations which tends to zero in CGAC180. The shoulder at 1165 cm^{-1}, which is more pronounced on CGACs spectra than on CAC spectrum, is attributed to the C–O stretching (1165 cm^{-1}) vibration of phenols, acids, ether and/or esters groups [33].

To conclude on IR characterization, the most important changes introduced by the increase of the impregnation ratio of coffee grounds from 30 to 180 wt.% are the development of carbonyl groups (~1700 cm^{-1}) as well as the increase of phosphorous groups content (1070–1080 cm^{-1}). Moreover, the surface chemistry is modified between CGAC120 and CGAC180: (1) decrease in intensity of the C–O–C band (at 1050 cm^{-1}); (2) decrease in intensity of the O–H bending band (at 1450 cm^{-1}) correlated with the content decrease of carboxylic and phenol groups reported in Table 5. All these modifications lead to an increase of the CGAC180 pH compared with the other CGAC prepared at lower content of phosphoric acid.

3.4. Dye adsorption

The adsorption isotherms of MB onto the activated carbons (CAC or CGACs) are type I (Fig. 8) suggesting that the adsorption occurs on specific sites forming a monolayer [34]. The higher the impregnation ratio of CGACs, the higher the adsorption capacity (q_m) of MB. The CAC shows twice as much adsorption uptake of MB (~360 mg g^{-1}) as CGAC180 (~175 mg g^{-1}). Good agreements of the adsorption isotherms of MB with the Langmuir equations ($R^2 > 0.99$) are found (Table 7).

The ratio between the surface area of material covered by MB (S_{MB}) and the BET specific surface areas (S_{BET}) of CGACs are given in Table 7. This coverage ratio is quite constant (50–60%) whatever the impregnation ratio (X_p) but not in agreement with the mesopores–macropores content which increases as X_p increases. This means that MB molecules do not fill all the wide mesoporous–macroporous volume of the CGAC120 and CGAC180. For CAC, the MB coverage ratio is higher than the

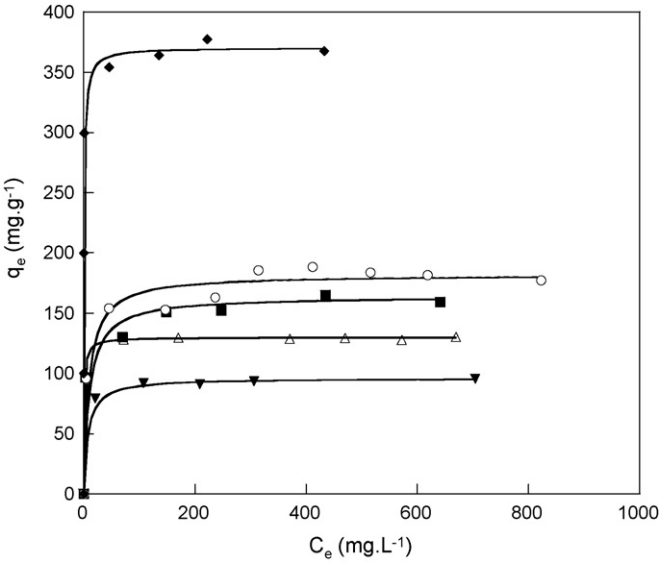

Fig. 8. Experimental adsorption isotherms at pH 6 and 25 °C of methylene blue on activated carbons: CGAC30 (▼), CGAC60 (△), CGAC120 (■), CGAC180 (○) and CAC (♦). Langmuir models (full lines).

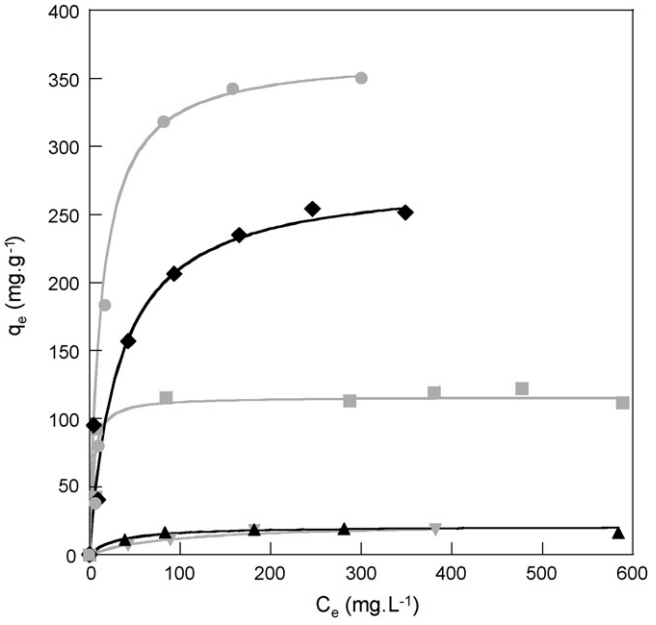

Fig. 9. Experimental adsorption isotherm at pH 4 and 25 °C of Nylosan Red (NR) on activated carbons; CGAC30 (▼), CGAC60 (▲), CGAC120 (■), CGAC180 (●) and CAC (♦) and corresponding Langmuir model fits (full line).

mesoporous–macroporous content indicating that part of micropores are occupied by MB molecules in agreement with the work of Graham [35] who mentioned a minimum pore size of 1.33 m required for MB adsorption and the study of Kasaoka et al. [36] who reported that adsorption can occur only as the pore diameter is about 1.7 times larger than the width of molecules (>1 nm for MB molecule). Thus, MB which is not to able to penetrate in the pores with diameter < 1.0 nm is assumed to access to wide micropores (namely supermicropores) in the CAC so that a highest adsorption uptake is observed for CAC compared to CGACs.

The adsorption can also be explained on the basis of an electrostatic interaction between the ionic dye molecule and the charged carbon substrate. At pH 6 where the MB adsorption isotherms were studied, the CGAC30, CGAC60 and CGAC120 activated carbons are negatively charged (pH > pH_{PZC} ~ 3.7) while the CGAC180 and CAC are positively charged (pH < pH_{PZC}). Though electrostatic repulsion between the MB cation (at pH 6) and CGAC180 (or CAC) should not favour adsorption; the highest adsorption uptake are measured for these carbons. Thus, the adsorption of MB cannot be only controlled by the electrostatic interactions. Indeed, Faria et al. [37] and Qian et al. [38] have shown that basic carbons still present better performances than acid carbons for adsorption of cationic dyes. This was attributed by Faria et al. [37] to the dispersive interactions between the delocalized π electrons on the surface of the basic activated carbons and the free conjugated electrons of the dye molecules.

In the literature, the basicity of activated carbons is described in term of delocalized π-electrons within the graphene layers which forms Lewis basic sites (electron donor). Leon y Leon et al. [39] have stated that protons could chemisorb on such sites *via* π-electrons carbon pair. The decrease in the π-electrons density on the graphene layers can be expected to result from the electron withdrawing effect of carboxylic and lactonic groups. Thus, in acidic carbons (CGAC30, CGAC60 and CGAC120), a part of the adsorption sites (basal sites) might be shifted from the π-electron graphene layer to the oxygenated functional groups at the edge of the layers which interact weakly with methylene blue molecules. To conclude, if the porous structure is accessible to MB as in CAC (presence of supermicropores and small mesopores), the more basic the activated carbon, the higher the MB adsorption uptake.

Table 8
Langmuir parameters of adsorption isotherms of Nylosan Red (NR) on activated carbons.

Activated carbon	Langmuir parameters	
	q_m (mg L^{-1})	k_L (L mg^{-1})
CGAC30	23	0.011
CGAC60	21	0.032
CGAC120	116	0.288
CGAC180	367	0.077
CAC	278	0.031

Fig. 9 shows that the adsorption isotherms of NR on the activated carbons at 25 °C (CGACs and CAC) are well fitted by a Langmuir equation (Table 8). By contrast with the MB adsorption, CGAC180 is better than CAC for NR adsorption.

The anionic character of NR is due to the presence of a sulfonate group (Fig. 1) of which the pK_a value is assumed to be negative,

Table 7
Langmuir parameters of the adsorption isotherms of methylene blue onto the activated carbons and the surface areas of materials covered by methylene blue molecules. The ratios of coverage of MB and of meso- and macro-pores with respect to the BET specific surface area are mentioned.

Activated carbon	Parameters of Langmuir model		Surface area covered by methylene blue	Methylene blue coverage ratio	Mesopore and macropore coverage ratio
	q_m (mg g^{-1})	k_L (L mg^{-1})	S_{MB} (m^2 g^{-1})	S_{MB}/S_{BET} (%)	S_{ext}/S_{BET} (%)
CGAC30	96.1	0.133	264	51	39
CGAC60	129.9	0.939	357	58	61
CGAC120	163.9	0.099	452	61	79
CGAC180	181.8	0.109	501	54	93
CAC	370.4	1.050	1021	71	56

as observed for p-toluenesulfonic acid ($pK_a = -2.8$). The $pK_1 = 6.8$ and the $pK_2 = 9.2$ determined by pHmetry (Table 1) correspond to the various acido-basic forms of the amine groups ($-NH_3^+/-NH_2$) and the hydroxyl groups ($-OH/-O^-$). At pH 4, the sulfonate group is anionic whereas the amine groups are assumed to be protonated, so that the whole dye molecule is positively charged. At the same pH, CGAC30, CGAC60 and CGAC120 are all negatively charged ($pH_{PZC} \sim 7$); whereas CGAC180 and CAC are positively charged (pH_{PZC} 7.4 and 9.8 respectively). Thus, the electrostatic attraction is higher for the acidic carbons ($X_p = 30–120$ wt.%) than for CGAC180 and CAC as their pH_{PZC} are 7.4 and 9.8 respectively. As a result, the knees of the Langmuir type adsorption isotherms (Fig. 9) are more pronounced following these trends: CGAC120 > CGAC180 > CAC; according to the strength of interaction between the carbon surface and NR following the decreasing order of the pH_{PZC} values. The values of the Langmuir constants k_L reported in Table 8 are in agreement with the same trend except for CGAC30 and CGAC60.

As previously mentioned with the MB dye, the adsorption is again governed by dispersive interactions by the porous volume of the carbons which is accessible to the dye molecule relatively to the adsorbate size porous volume of materials. According to its molecular size, this dye can be included in a sphere of minimum diameter ~2.1 nm. This means that mesopores are required to adsorb NR.

As CGAC30 and CGAC60 show very similar DFT PSDs (Fig. 4), their NR adsorption isotherms are practically superimposed (Fig. 9). These PSDs display very small amount of pores close to the dimension of dye molecule. This explains the absence of square profile on both isotherms, despite of the high electrostatic interaction with the dye.

The NR adsorption capacity is directly proportional to the mesoporous volume which corresponds to pore diameter higher than ~3 nm (accessible to NR molecule). This volume can be estimated roughly from the PSD computed from DFT (Fig. 4). Fig. 4 shows that this appropriate mesoporous volume is clearly larger for CGAC180 than for CAC and also higher for CAC than for CGAC120. Thus, the carbons can be classified by their NR adsorption uptake: CGAC180 > CAC > CGAC120 in agreement with the adsorption experimental results (Fig. 9).

4. Conclusion

The thermal treatment at 450 °C of coffee bean grounds impregnated with phosphoric acid yields to activated carbons of which porous structure and surface chemistry can be easily controlled by simply varying the impregnation ratio. Low impregnation ratios ($X_p <$ ~60 wt.%) lead to acidic microporous carbons ($pH_{PZC} \sim 3.7$) with almost no mesopores and low surface areas ($S_{BET} \sim 600\ m^2\ g^{-1}$). As increasing the impregnation ratio from 60 to 180 wt.%, thermogravimetric analyses and elemental analyses showed that the content of oxygenated surface groups was reduced from 20 to 13 wt.%. At impregnation level as high as 180 wt.%, the acidic surface shifts to neutral (pH_{PZC} 7.4) because of the decrease in amount of carboxylic and phenol groups and the development of carbonyl surface groups observed by IR spectroscopy and "Boehm titrations". The use of high impregnation ratio (CGAC180) allows to obtain exclusively mesoporous carbons with surface areas as high as $925\ m^2\ g^{-1}$ and pore volume as large as $0.7\ cm^3\ g^{-1}$. Due to its high mesopore content, this latter activated carbon appears as a good adsorbant for organic pollutants of middle molecular size (>2 nm). For instance, the adsorption uptake of Nylosan Red N-2RBL (anionic dye of diameter ~2 nm) onto this carbon is 1.75-fold higher than that of a commercial activated carbon ($S_{BET} \sim 1400\ m^2\ g^{-1}$) because of an appropriate pore size distribution (mainly mesopores of diameter wider than 3 nm) and a neutral surface chemistry.

References

[1] M. Hirata, N. Kawasaki, T. Nakamura, K. Matsumoto, M. Kabayama, T. Tamura, I. Tanada, Adsorption of dyes onto carbonaceous materials produced from coffee grounds by microwave treatment, J. Colloid Interface Sci. 254 (2002) 17–22.

[2] Y. Guo, D.A. Rockstraw, Physicochemical properties of carbons prepared from pecan shell by phosphoric acid activation, Bioresour. Technol. 98 (2007) 1513–1521.

[3] M.J.B. Evans, E. Halliop, J.A.F. MacDonald, The production of chemically-activated carbon, Carbon 37 (1999) 269–274.

[4] F. Suárez-García, A. Martínez-Alonso, J.M.D. Tascón, Porous texture of activated carbons prepared by phosphoric acid activation of apple pulp, Carbon 39 (2001) 1103–1116.

[5] B.S. Girgis, A.-N.A. El-Hendawy, Porosity development in activated carbons obtained from date pits under chemical activation with phosphoric acid, Micropor. Mesopor. Mater. 52 (2002) 105–117.

[6] G. Rodríguez, A. Lama, R. Rodríguez, A. Jiménez, R.L. Guillén, J. Fernández-Bolaños, Olive stone an attractive source of bioactive and valuable compounds, Bioresour. Technol. 99 (2008) 5261–5269.

[7] A. Attia, B.S. Girgis, N.A. FathyRole, Removal of methylene blue by carbons derived from peach stones by H_3PO_4 activation: batch and column studies, Dyes Pigments 76 (2008) 282–289.

[8] A.-N.A. El-Hendawy, S.E. Samara, B.S. Girgis, Adsorption characteristics of activated carbons obtained from corncobs, Colloids Surf. A: Physicochem. Eng. Aspects 180 (2001) 209–221.

[9] M.C. Baquero, L. Giraldo, J.C. Moreno, F. Suarez-Garcıa, A. Martınez-Alonso, J.M.D. Tascon, Activated carbons by pyrolysis of coffee bean husks in presence of phosphoric acid, J. Anal. Appl. Pyrolysis 70 (2003) 779–784.

[10] R. Tsunoda, T. Ozawa, J.-I. Ando, Ozone treatment of coal- and coffee grounds-based active carbons: water vapor adsorption and surface fractal micropores, J. Colloid Interface Sci. 205 (1998) 265–270.

[11] T. Nakamura, T. Tokimoro, N. Kawasaki, S. Tanada, Decolorization of acidic dye by charcoal from coffee grounds, J. Health Sci. 49 (2003) 520–523.

[12] A. Namane, A. Mekarzia, K. Benrachedi, N. Belhaneche-Bensemra, A. Hellal, Determination of the adsorption capacity of activated carbon made from coffee grounds by chemical activation with $ZnCl_2$ and H_3PO_4, J. Hazard. Mater. B119 (2005) 189–194.

[13] E. Yagmur, M. Ozmak, Z. Aktas, A novel method for production of activated carbon from waste tea by chemical activation with microwave energy, Fuel 87 (2008) 3278–3285.

[14] M. Valix, W.H. Cheung, G. McKay, Preparation of activated carbon using low temperature carbonisation and physical activation of high ash raw bagasse for acid dye adsorption, Chemosphere 56 (2004) 493–501.

[15] J. Laine, A. Calafat, M. Labady, Preparation and characterization of activated carbons from coconut shell impregnated, Carbon 27 (1989) 191–195.

[16] P.J.M. Suhas, M.M.L. Carrott, R. Carrott, Lignin—from natural adsorbent to activated carbon: a review, Bioresour. Technol. 98 (2007) 2301–2312.

[17] M. Jagtoyen, F. Derbyshire, Activated carbons from yellow poplar and white oak by H_3PO_4 activation, Carbon 36 (1998) 1085–1097.

[18] O. Ioannidou, A. Zabanistou, Agricultural residues as precursors for activated carbon production—a review, Renew. Sustain. Energy Rev. 11 (2007) 1966–2005.

[19] H. Marsh, F. Rodriguez-Reinoso, Activated Carbon, Elsevier Ltd., Oxford, 2006, pp. 322–349.

[20] A. Nakanishi, M. Tamai, N. Kawasaki, T. Nakamura, M. Araki, S. Tanada, Characterization of water adsorption onto carbonaceous materials produced from food wastes, J. Colloid Interface Sci. 255 (2002) 59–63.

[21] C.A. Toles, W.E. Marshall, M.M. Johns, L.H. Wartelle, A. McAloon, Acid-activated carbons from almond shells: physical, chemical and adsorptive properties and estimated cost of production, Bioresour. Technol. 71 (2000) 87–92.

[22] M Molina-Sabio, F. Rodrıguez-Reinoso, Role of chemical activation in the development of carbon porosity, Colloids Surf. A: Physicochem. Eng. Aspects 241 (2004) 15–25.

[23] M.V. Lopez-Ramon, F. Stoeckli, C. Moreno-Castilla, F. Carrasco-Marin, On the characterization of acidic and basic surface sites on carbons by various techniques, Carbon 37 (1999) 1215–1221.

[24] H.P. Boehm, Surface oxides on carbon and their analysis: a critical assessment, Carbon 40 (2) (2002) 145–149.

[25] F. Rouquerol, J. Rouquerol, K. Sing, Adsorption by Powders and Porous Solids. Principles, Methodology and Applications, Academic Press, London, 1999.

[26] E.P. Barrett, L.J. Joyner, P.H. Halenda, The determination of pore volume and area distribution on porous solids I: computation from nitrogen isotherms, J. Am. Chem. Soc. 73 (1951) 373–380.

[27] C. Pelekani, V.L. Snoeyink, Competitive adsorption between atrazine and methylene blue on activated carbon: the importance of pore size distribution, Carbon 38 (2000) 1423–1436.

[28] P.T. Hang, G.W. Brindley, Methylene blue absorption by clay minerals. Determination of surface areas and cation exchange capacities, Clays Clay Miner. 18 (1970) 203–212.

[29] M. Molina-Sabio, F. Caturla, F. Rodrıguez-Reinoso, Influence of the atmosphere used in carbonization of phosphoric acid impregnated peach stones, Carbon 33 (1995) 1180–1182.

[30] F. Caturla, M. Molina-Sabio, F. Rodrigues-Reinoso, Preparation of activated carbon by chemical activation with $ZnCl_2$, Carbon 29 (7) (1991) 999–1007.

[31] A.M. Puziy, O.I. Poddubnayaa, A. Martınez-Alonso, F. Suarez-Garcıa, J.M.D. Tascon, Synthetic carbons activated with phosphoric acid I. Surface chemistry and ion binding properties, Carbon 40 (2002) 1493–1505.
[32] S. Bourbigot, M. Le Bras, R. Delobel, Carbonization mechanisms resulting from intumescence. II. Association with an ethylene terpolymer and the ammonium polyphosphate-pentaerythritol fire retardant system, Carbon 33 (3) (1995) 283–294.
[33] J. Coates, Interpretation of infrared spectra, a practical approach, in: R.A. Meyers (Ed.), Encyclopedia of Analytical Chemistry, Chichester John Wiley & Sons Ltd., 2000, pp. 10815–11037.
[34] Y.R. Lin, H. Teng, Mesoporous carbons from waste tire char and their application in wastewater discoloration, Micropor. Mesopor. Mater. 54 (2002) 167–174.
[35] D. Graham, Characterization of physical adsorption systems III. The separate effects of pore size and surface acidity upon the adsorbent capacities of activated carbons, J. Phys. Chem. 59 (8) (1955) 896–900.
[36] S. Kasaoka, Y. Sakata, E. Tanaka, R. Naitoh, Preparation of activated fibrous carbon from phenolic fabric and its molecular sieve properties, Int. Chem. Eng. 29 (1) (1989) 101–114.
[37] P.C.C. Faria, J.J.M. Orfao, M.F.R. Pereira, Adsorption of anionic and cationic dyes on activated carbons with different surface chemistries, Water Res. 38 (2004) 2043–2052.
[38] Q. Qian, M. Machida, H. Tatsumoto, Textural and surface chemical characteristics of activated carbons prepared from cattle manure compost, Waste Manage. 28 (2008) 1064–1071.
[39] C.A. Leon y Leon, J.M. Solar, V. Calemma, L.R. Radovic, Evidence for the protonation of basal plane sites on carbon, Carbon 30 (1992) 797–811.